

## Article

# Hydrodynamic Hysteresis and Solute Transport in Agglomerated Heaps under Irrigation, Stacking, and Bioleaching Controlling

Leiming Wang<sup>1,2,3,4,5</sup> , Shenghua Yin<sup>1,2,\*</sup>, Xuelan Zhang<sup>6</sup>, Zepeng Yan<sup>1,2</sup> and Wensheng Liao<sup>7</sup>

<sup>1</sup> Key Laboratory of Ministry of Education for High-Efficient Mining and Safety of Metal, University of Science and Technology Beijing, Beijing 100083, China

<sup>2</sup> School of Civil and Environment Engineering, University of Science and Technology Beijing, Beijing 100083, China

<sup>3</sup> State Key Laboratory of Coal Mine Resources and Safety Mining, China University of Mining and Technology, Xuzhou 221116, China

<sup>4</sup> State Key Laboratory Safety and Health for Metal Mines, Sinosteel Maanshan General Institute of Mining Research Co., Ltd., Maanshan 243000, China

<sup>5</sup> Key Laboratory of Green Chemical Engineering Process of Ministry of Education, Wuhan University of Technological, Wuhan 430205, China

<sup>6</sup> School of Mathematics and Physics, University of Science and Technology Beijing, Beijing 100083, China

<sup>7</sup> Beijing Research Institute of Chemical Engineering Metallurgy, Beijing 101149, China

\* Correspondence: [ustb\\_ymh@163.com](mailto:ustb_ymh@163.com); Tel.: +86-138-1166-8481

**Abstract:** Hydrodynamic hysteresis exists widely in agglomerated heaps with well-developed intrapores, and it directly affects solute transports and bioleaching reaction. In this paper, the dynamic liquid retention behavior under different heap porosity and irrigation condition is quantified via a novel real-time, in-situ liquid retention characterizing system (RILRCS), and the potential effects of initial liquid retention on solute transport and leaching reaction are carefully discussed. The results show that the immobile liquid is dominant in agglomerated heaps. The ratio of immobile and mobile liquid ( $\eta$ ) dynamically changes due to mineral dissolution and new flow path appearances. The  $\eta$  normally increases and mobile liquid occupies a higher proportion due to acidic leaching reactions, especially at a smaller  $R_g$  (10.32 mm) and a larger  $u$  (0.10 mm/s). The dynamic liquid retention is more sensitive to the diameter of packed feeds ( $R_g$ ) and superficial flow rate ( $u$ ) instead of leaching reactions. This might be because the damage of leaching reaction on minerals pores/voids is limited and cannot extensively change the potential pore channels or fluid flow paths. Based on pulse tracing and conductivity tests, we reveal that the solute resides longer under a slower  $u$  and smaller packed  $R_g$  condition, which corresponds well with desirable copper leaching efficiency. Specifically, the liquid hysteresis behavior is more obvious at a lower  $u$  (0.01 mm/s) and smaller  $R_g$  (10.32 mm). This paper gives a good reference to ascertain the liquid retention and hydrodynamic hysteresis and promote mineral leaching performance.

**Keywords:** agglomerated heap; liquid retention; hysteresis behavior; solute transport; fluid flow



**Citation:** Wang, L.; Yin, S.; Zhang, X.; Yan, Z.; Liao, W. Hydrodynamic Hysteresis and Solute Transport in Agglomerated Heaps under Irrigation, Stacking, and Bioleaching Controlling. *Minerals* **2022**, *12*, 1623. <https://doi.org/10.3390/min12121623>

Academic Editor: Luis A. Cisternas

Received: 8 October 2022

Accepted: 10 December 2022

Published: 16 December 2022

**Publisher's Note:** MDPI stays neutral with regard to jurisdictional claims in published maps and institutional affiliations.



**Copyright:** © 2022 by the authors. Licensee MDPI, Basel, Switzerland. This article is an open access article distributed under the terms and conditions of the Creative Commons Attribution (CC BY) license (<https://creativecommons.org/licenses/by/4.0/>).

## 1. Introduction

Low-grade minerals, waste ores, and even e-wastes are diffusely deposited in the earth [1,2]. These secondary recyclable resources require low-cost, environmentally-friendly, and efficient mining methods. Since 1980s, heap leaching, which crushes ores and then packs them in heaps [3,4], has been successfully industrialized in the United States, Canada, Chile, South Africa, China, and other countries. The agglomeration, as an effective pre-treatment method of crushed ores, is widely utilized in the heap leaching of copper oxides, copper sulfides, laterite nickels, and uranium minerals.

The experimental agglomeration refers to the procedure of using chemical binders to adsorb and bond crushed ores and fine powders to form well-shaped agglomerations (WAs), which could obviously ameliorate pore structure, fluid flow, and solute dispersion [5].

Similar with crushed ore heaps, both the unsaturated and saturated condition exist in agglomerated heaps simultaneously [6,7]. The liquid hysteresis behavior in unsaturated beds respectively packed by solid glass beads, crushed ores, and agglomerations are comparatively discussed. Recently, some novel detecting methods such as computer tomography (CT), magnetic resonance image (MRI), and particle tracking velocimetry (PIV) have been introduced to describe the liquid retention behavior. Although these undisturbed methods are mostly short-term and high cost, studies have indicated that developing differences of intra-aggregate and inter-aggregate porosity is an essential reason for differences in liquid hysteresis. Due to well-developed intra-particle pores and voids [8], the liquid retention and hysteresis appeared more easily than for the crushed ore heaps, which is regarded as one of the essential factors leading to desirable leaching efficiency. The fluid flow is closely related to the formation of flow paths and fluid dispersion in unsaturated heaps [9,10]. In addition to the superficial flow rate, the fluid flow pattern is also related to the flow pipe diameter, fluid viscosity, and density. The flow pattern in unsaturated crushed ore/agglomerated heap is commonly shown as laminar flow where the flow rate is higher in the central part of flow tubes.

It is impossible for the solute (including valuable metallic/non-metallic ions, soluble oxygen, etc.) to be independent of the leaching system and its transport process must rely on liquid medium. A consensus has been developing that the solute consistently existed in the reactive fluid inside unsaturated heaps, and solute transport is closely related to solution flow. The efficiency of solute transports represents the ion exchange rate at the reaction interface and limits the mineral dissolution to some extent. Specifically, the solute transport areas in the unsaturated heaps are closely related to mobile liquid (mainly shown as preferential flow), while the solute transport efficiency is closely related to immobile liquid (mainly shown as stagnant flow). The existing research shows that there are two key star-like inter-particle pores and intra-particle pores in the ore heap, and solute transport widely exists in the inter-particle pores with solution as the key medium [11,12]. These solute/mass (including solute oxygen, metallic ions, etc.) transports could be affected by channeling tortuosity [13,14], contact angle at the solid-fluid interface [15], and the diameter of pore throat [16,17]. In the heap heterogeneous, the segregation and stratification phenomenon appeared widely [18]. This could also be quantitatively characterized by detecting liquid holdup difference from macro-scope [19]. Caused by the complex hydraulic conductivity and hysteresis in unsaturated heaps, it is hard to quantitatively characterized solute transport [20,21]. To describe the solute transport and liquid retention behavior of different unsaturated porous systems, previous studies have mainly focused on numerical simulation to characterize the solute transport process under the effect of different porosity and irrigation condition. Except for the mathematical modeling studies mentioned above, hydrodynamics features in fluid flow and solute transport in unsaturated porous heaps are explored via column system. Some detection methods including calibration solute tracing and overflow conductivity measuring are utilized to quantify the solute transport behavior, and discuss the potential effect of liquid hysteresis on mass transfer in the minerals interface [22]. In addition, Neethling's team of Imperial College London innovatively used the suspension force measurement method to monitor the liquid holding behavior of the static ore particle pile system. Some computer tomography, nuclear magnetic resonance, and other techniques have also been applied to the liquid holding characteristics of unsaturated porous media stacking heap [23–25], but the above research findings are more static and transient without considering mineral leaching. Despite this, there are still few studies that both consider liquid hysteresis and solute transport in agglomerated leaching condition, leading to a research gap regarding a deep understanding of how agglomerated heaps enhance mineral leaching and solute transport intensification [26–28].

In this paper, using a novel developed in-situ, real-time liquid retention characterizing experimental system, the fluid flow, dynamic liquid retention, and hysteresis behavior in unsaturated agglomerated heaps are effectively discussed. To better show the potential connection between liquid retention and mass transfer of agglomerated heap leaching sys-

tem, the dynamic liquid retention is quantitative by the liquid holdup value  $\theta$ , the residual liquid holdup value  $\theta_{residual}$ , and the ratio of immobile and mobile liquid  $\eta$ ; the dynamic solute transport in agglomerated heaps is quantitatively described by fluid parameters, such as overflow the overflow conductivity, and residual time distribution (RTD). The research measures and findings in this paper could promote the understanding of the dynamic liquid retention and hysteresis behavior in agglomerated heaps under different inter-aggregate porosity (comparing diameter of WAs), intra-particle porosity (comparing feeds with same diameters), and superficial flow rate condition.

## 2. Materials and Methods

### 2.1. Ore Samples and Its Agglomeration Condition

The ore feeds are sampled from copper sulfides mines in China. The valuable copper minerals mainly are copper sulfides (chalcocite and chalcopyrite, etc.) and copper oxides (malachite, etc.). The total mass fraction of  $Cu^{2+}$  is 0.70% (free copper oxides is 5.71%, primary/secondary copper sulfides occupied 92.86%), the gangue minerals is mainly quartz. The agglomerated condition is set as: rolling speed is 80 rpm, inclined angle is  $30^\circ$ , curing time is 7 days, and chemical binder is 9.3% sulfuric acid solution. The diameter of 50% crushed ore feeds is less than 2 mm, and 35% is less than 1 mm. The diameter of 80% WAs is larger than 10 mm. The difference of particle bonding collision in agglomeration procedure is not considered in this paper.

### 2.2. Real-Time, In-Situ Liquid Retention Characterizing System (RILRCS)

To quantitatively describe the dynamic liquid retention and solute transports in agglomerated heaps, a novel real-time, in-situ liquid retention characterizing system (RILRCS) is well developed (Figure 1). Taking the functionality as evaluation factors, the structure of RILRCS is divided into (Figure 1a): liquid irrigating (9, 10, 11, 13, 14, 15, 16, 17, 18), tension measuring (5, 6), data visualizing (8), and supporting (1, 2, 3, 4, 7, 12) systems.

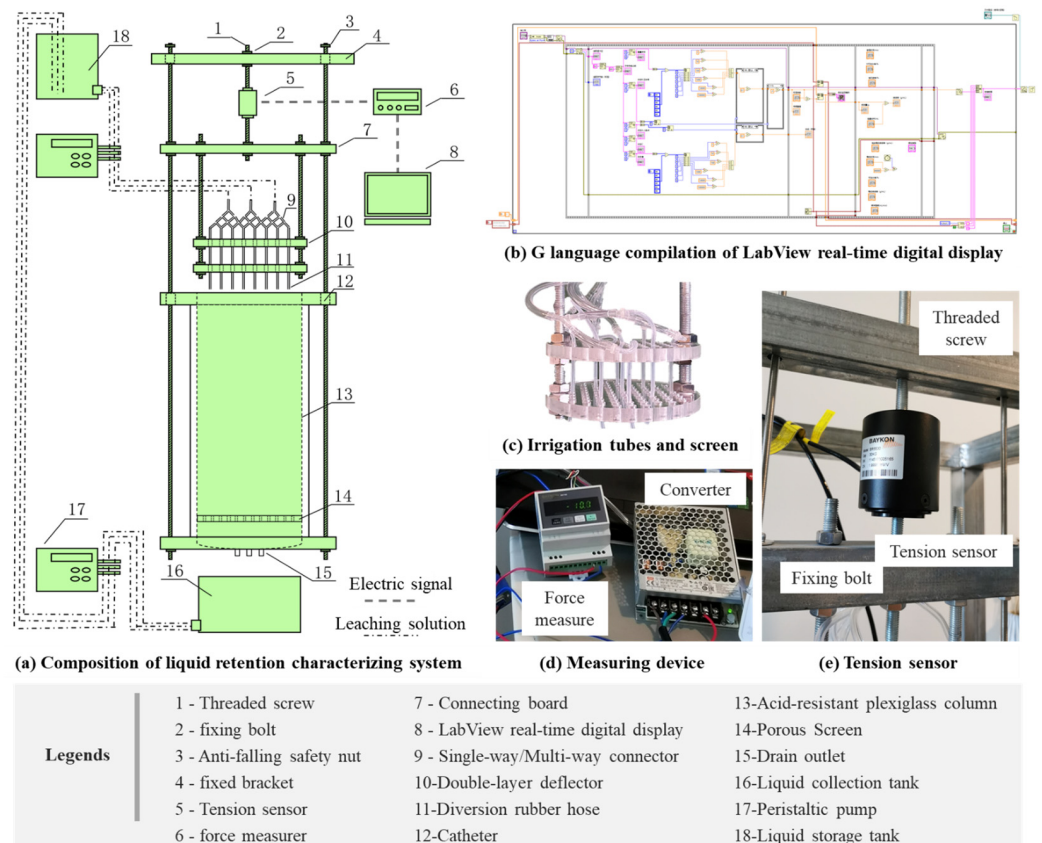


Figure 1. Scheme of novel Real-time, In-situ Liquid Retention Characterizing System (RILRCS).

The RILRCS idea is to use a tension sensor (Figure 1e) to monitor and converted dynamical liquid retention signal into electrical signal by force measurer and converter (Figure 1d). The effective measuring range of liquid retention is 30 kg, test accuracy is 0.001 kg. The A/D conversion rate is 200 times/s and counting step is 15 s. The electrical signals are compiled by LABVIEW and graphical language (Figure 1b), eventually obtaining the liquid holdup ( $\theta$ ), residual liquid holdup ( $\theta_{residual}$ ), and ratio of immobile and mobile liquid ( $\eta$ ). The dripping irrigation uses the uniform vertical hoses and glass porous board (Figure 1c). The pulse conductivity of overflow in liquid collection tank (Figure 1a) is measured regularly.

### 2.3. Experimental Scheme and Design

This paper utilizes column leaching experiment (CLE) and pulse tracing experiment (PTE) to study the dynamic liquid retention behavior, solute transport, and its influencing factors in agglomerated heaps. The detailed experimental scheme and key parameters are shown in Table 1. The dynamic liquid retention in leaching process is detected via RILRCS. The key parameters of overflow, namely  $\text{Cu}^{2+}$  concentration, pH/Eh, and bacterial concentration, are measured. The influencing factors are described: (1) packed feed types (solid glass beads, crushed ore, and Was), (2) geometric mean diameter of agglomerations (10.32, 16.02, and 24.36 mm), and (3) superficial flow rate (0.01, 0.02, 0.05, and 0.10 mm/s), respectively. Different WAs feeds and irrigation conditions were set up.

**Table 1.** Experimental scheme of pulse tracing and column leaching in this paper.

Experiment	Factors	Packed Feed Type	Geometric Mean Diameter (mm)	Superficial Flow Rate (mm/s)
Pulse Tracing Experiment (PTE)	Packed feed types	Solid glass beads	16.02	0.10
		Crushed ore	16.02	0.10
		Well-shaped agglomerations (WAs)	16.02	0.10
	Geometric mean diameter of packed feeds	WAs	10.32	0.10
		WAs	16.02	0.10
		WAs	24.36	0.10
	Superficial flow rate (Irrigation rate)	WAs	16.02	0.01
		WAs	16.02	0.02
		WAs	16.02	0.05
		WAs	16.02	0.10
Column Leaching Experiment (CLE)	Geometric mean diameter of packed feeds	WAs	10.32	0.10
		WAs	16.02	0.10
		WAs	24.36	0.10
	Superficial flow rate (Irrigation rate)	WAs	16.02	0.01
		WAs	16.02	0.02
		WAs	16.02	0.05
		WAs	16.02	0.10

In the CLE, the WAs are artificially dumped and packed the agglomerated heaps. Then the acidic solution is irrigated from the top of packed agglomerated heaps, the bacterial concentration, pH/Eh value, and cupric ions concentration (copper extraction rate) of overflow are detected regularly. The basic liquid medium is no-ferrous 9K solution containing 3.0 g  $(\text{NH}_4)_2\text{SO}_4$ , 0.5 g  $\text{K}_2\text{HPO}_4$ , 0.1 g KCl, 0.5 g  $\text{MgSO}_4 \cdot 7\text{H}_2\text{O}$ , and 0.01 g  $\text{Ca}(\text{NO}_3)_2$  per liter. The initial pH value is set as 2.00. The functional leaching micrograms are injected and domesticated in leaching medium. The dominant bacteria species are

*Acidithiobacillus ferrooxidans* (*A.f*) and *Acidophilus thiooxidans* (*A.t*). The initial total bacterial concentration is roughly  $2.0 \times 10^6$  cell/mL, the environmental temperature is  $28 \pm 2^\circ$ .

In the PTE, to detect the solute transport under different initial liquid retention conditions, the tracer ion is thought as solute ions of valuable minerals reserved in the ore samples. The conductivity value of overflow contained tracer ions is continuously detected by conductivity sensor. The  $4.00 \text{ mol/dm}^3$  NaCl solution is used as the experimental tracer, and this NaCl tracer was injected once in a pulse (shown in Figure 2), with an injection volume of 0.05 mL. This pulse injection adopts a single dipper head. The overflow conductivity is measured by the inserted sensors, and the residual time distribution (RTD) is calculated according to previous similar studies. The residence, spreading, and hysteresis behavior of solute (tracer ions) in agglomerated heaps are carefully discussed.

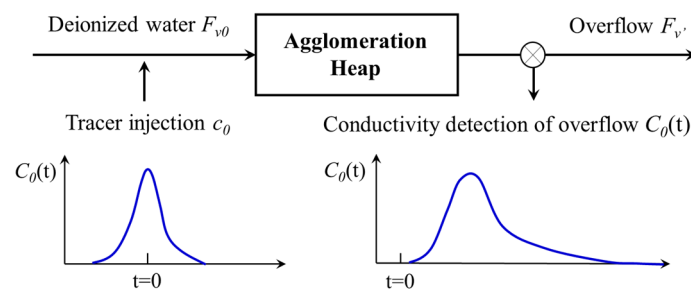


**Figure 2.** Experimental scheme of conductivity pulse tracer method using NaCl solution.

#### 2.4. Key Parameters of Liquid Retention and Solute Transports

##### 2.4.1. Liquid Holdup ( $\theta$ ) and Residual Liquid Holdup ( $\theta_{residual}$ )

In irrigation and drainage process, the agglomerated heaps reach static, and residual steady-state of liquid retention, which is corresponding with liquid holdup ( $\theta$ , %) and residual liquid holdup ( $\theta_{residual}$ , %), respectively. As described in [29], two key parameters are calculated by Equations (1) and (2).

$$\theta = \frac{\int (v_{in} - v_{out}) dt}{V} = \frac{v_{in}t - m_{out}/\rho}{V} \tag{1}$$

$$\theta_{residual} = \frac{V_{steady} - \int (v_{out})dt}{V} = \frac{\theta V - m_{out}/\rho}{V} = 1 - \frac{m_{out}}{V\rho} \tag{2}$$

where  $v_{in}$  is flow rate in,  $v_{out}$  is flow rate out,  $m_{out}$  is mass of liquid flow out, and  $\rho$  is liquid density. The immobile and mobile liquid co-existed in flow paths and stagnant areas of agglomerated heap. To evaluate existing status of liquid (leaching solution) reserved in the agglomerated heaps, the ratio of immobile liquid and mobile liquid ( $\eta$ ) is utilized, which could be calculated by Equation (3).

$$\eta = \frac{\theta_{residual}}{\theta - \theta_{residual}} \tag{3}$$

##### 2.4.2. Solute Transport and Resident Parameters

The solute transport in agglomerated heap relies on liquid dispersion, which is heavily affected by heap porosity and liquid retention. The hydrodynamic diffusion coefficient  $D$  is the sum of effective molecular diffusion  $D_m$  and mechanical diffusion  $D_h$  (Equation (4)). The two diffusion processes cannot exist independently.

$$D = D_m + D_h = D_m + \lambda v^{n_0} = D_w \tau_l + \lambda v^{n_0} \tag{4}$$

wherein the  $D_h$  mechanical diffusion may be expressed as  $\lambda v^{n_0}$ . The  $\lambda$  is the scattering coefficient,  $n_0$  is an empirical constant,  $v$  is the pore water velocity,  $\theta$  is liquid holdup. The relationship of tracer conductivity and spray time curve  $C(t)$  can be obtained by PTE.

The conductivity distribution of the overflow water containing the tracer at the outlet is integrated and normalized, as shown in Equation (5).

$$E(t) = \frac{C(t)}{\int_0^\infty C(t) dt} \tag{5}$$

The residence time distribution (RTD) ranges from 0 to 1, representing the fraction of salt tracers whose residence time is less than a specific value. To better compare the solute transports under different liquid holdup conditions, take mean residence time ( $t_R$ ) as an indicator, as shown in Equation (6).

$$t_R = \int_0^\infty t E(t) dt = \int_0^\infty t \frac{C(t)}{\int_0^\infty C(t) dt} dt \tag{6}$$

### 3. Results and Discussion

#### 3.1. Key Parameters under Geometric Mean Diameter ( $R_g$ ) and Superficial Flow Rate ( $u$ )

##### (1) Cupric ionic concentration/copper extraction rate

The liquid (leaching solution), which contains types of metallic ions, continuously and disorderly spreads in the irrigation or drainage process of heap leaching operations. The leaching medium and feed diameter influence leaching kinetics of minerals dissolution. Thus, the column leaching conducted here is aimed at discussing the effect of initial liquid retention on leaching reaction. Figure 3 shows the relationship between leaching time and copper extraction rate under different geometric mean diameter ( $R_g$ , mm) and superficial flow rate ( $u$ , mm/s).

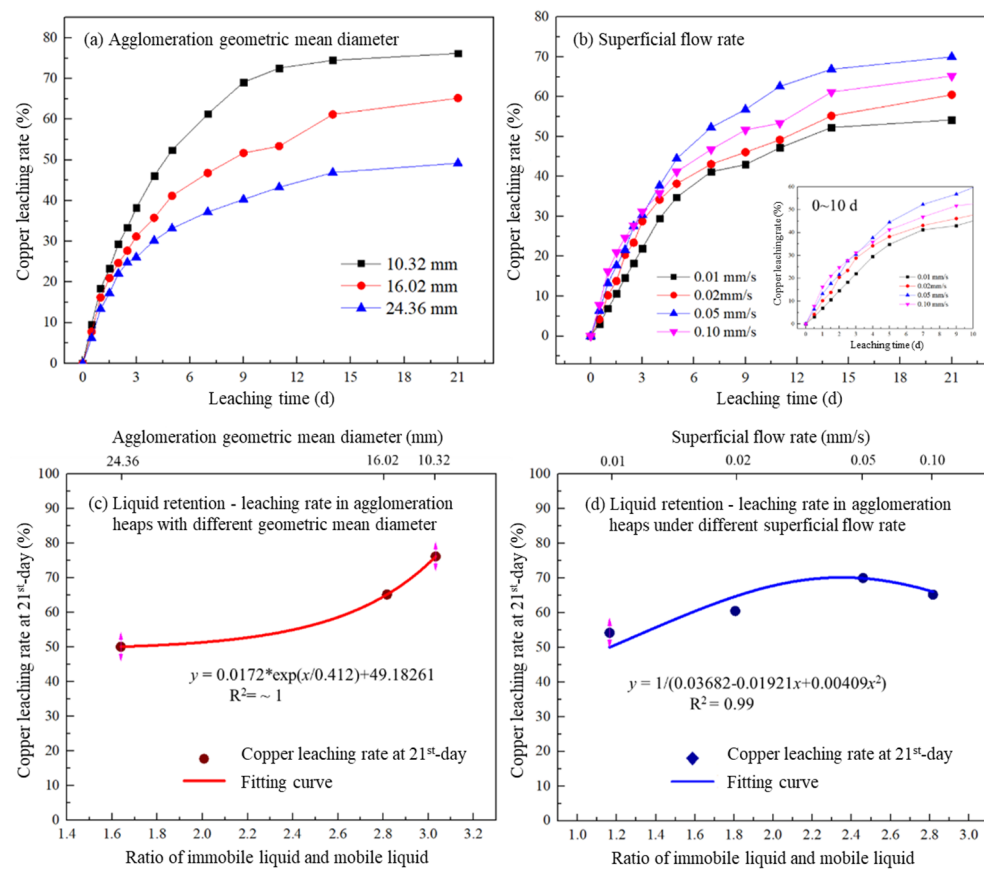


**Figure 3.** Copper leaching rate with leaching time under different packed and irrigation condition.

Due to a larger specific surface area, a better leaching reaction interface is provided in fine-grained (10.32 mm) agglomerated heaps where the peak copper extraction rate is

76.2%, which is much higher than 49.2% of coarse-grained (24.36 mm) agglomerated heaps (Figure 3a). For the copper sulfides leaching, it is known that its leaching kinetics could be roughly divided into two stages: the first stage is  $\text{Fe}^{3+}$  diffusion through the product layers controlled by solute concentration and temperature, which could correspond with the first 5 leaching days in this paper; the second stage is mainly controlled by mineral decomposition and  $\text{Fe}^{2+}$  reduction, which could corresponded with the 5–12 leaching days. In leaching solution, the reserved ferric ion ( $\text{Fe}^{3+}$ ) is reduced to ferrous ions ( $\text{Fe}^{2+}$ ) participated with oxygen and *A.f* bacteria, the  $\text{S}^{2-}$  is oxides to sulfate ions by *A.t* bacteria. To deeply understand leaching reaction under different effects of influencing factors, the chemical leaching reaction of the majority copper sulfide mineral compositions (including of chalcocite, covellite, and chalcopyrite) is simply shown in Equations (7)–(9), respectively.

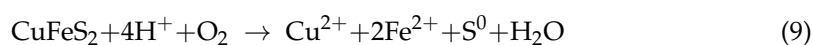
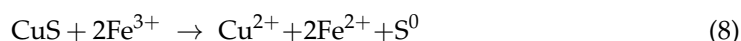
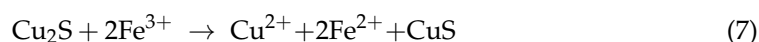


Figure 3b shows that the cupric ions are released to liquid in leaching process, and the mineral dissolution is desirable under 0.05 mm/s irrigation condition. When the agglomerated leaching is operated for 21 days, the peak value of copper extraction rate is 70.0% (at 0.05 mm/s), which is much higher than 54.2% (0.01 mm/s). As Figure 3c shows, accompanied with the increase of peak copper extraction rate under different  $R_g$  condition, the  $\eta$  tends to increase as well. In contrast, the peak value of copper extraction rate is obtained at 0.05 mm/s instead of 0.10 mm/s (Figure 3d). This means that for continuously increasing  $u$ , the solute diffusion and minerals dissolution in agglomerated heaps cannot be linearly improved. This fact might be caused by the recognition that most liquid and solute transport is conducted via preferential flow paths under an excessive high superficial flow rate [30]. The detailed liquid retention will be discussed below.

## (2) Bacterial concentration

The bacterial concentration in liquid medium keeps changing dynamically, and closely corresponds with sulfide mineral dissolution and reactions. Figure 4 shows the relationship between leaching time and bacterial concentration under the different initial liquid retention condition. Figure 4a,b infer that the initial liquid retention, which is designed by different packed and irrigation condition, could clearly affect the leaching efficiency. The bacterial concentration obviously increased from  $2.0 \times 10^6$  cells/mL to around  $1.6 \times 10^8$  cells/mL in the first 10 days, the peak bacterial concentration is roughly  $1.75 \times 10^8$  cells/mL obtained at 0.05 mm/s or using 10.32 mm WAs; then the bacterial apoptosis gradually appears to be caused by leaching environment deteriorations. In the agglomerated heaps packed by 24.36 mm WAs, the bacterial concentration decreases from  $1.16 \times 10^8$  cells/mL (at 14 days) to  $1.06 \times 10^8$  cells/mL (at 21 days). It could be explained that after a longer period of bioleaching reaction, the crusts composited by amounts of passivation products widely attached on the mineral surface, which fill pores/voids and seriously restrict the continuation of bioleaching reactions. Further, the changes of peak bacterial concentration with the  $\eta$  in Figure 4c,d correspond well with copper extraction rate (Figure 3), which also follows the close relationship between copper extraction rate and bacterial concentration. In other words, a desirable bacterial concentration is obtained by using small-diameter WAs or appropriate high  $u$ , resulting in a higher copper leaching efficiency.

## (3) pH/Eh value

The copper sulfide bio-/chemical leaching is a complex chemical reaction commonly occurring in acidic aqueous medium. The oxidation reduction potential (ORP) is closely related to soluble oxygen, and is also affected by the ratio of ferrous and ferric concentration [31]. Figure 5 shows that, regardless of  $R_g$  or  $u$ , the oxidation reduction potential (ORP, Eh) is higher when pH value is lower.

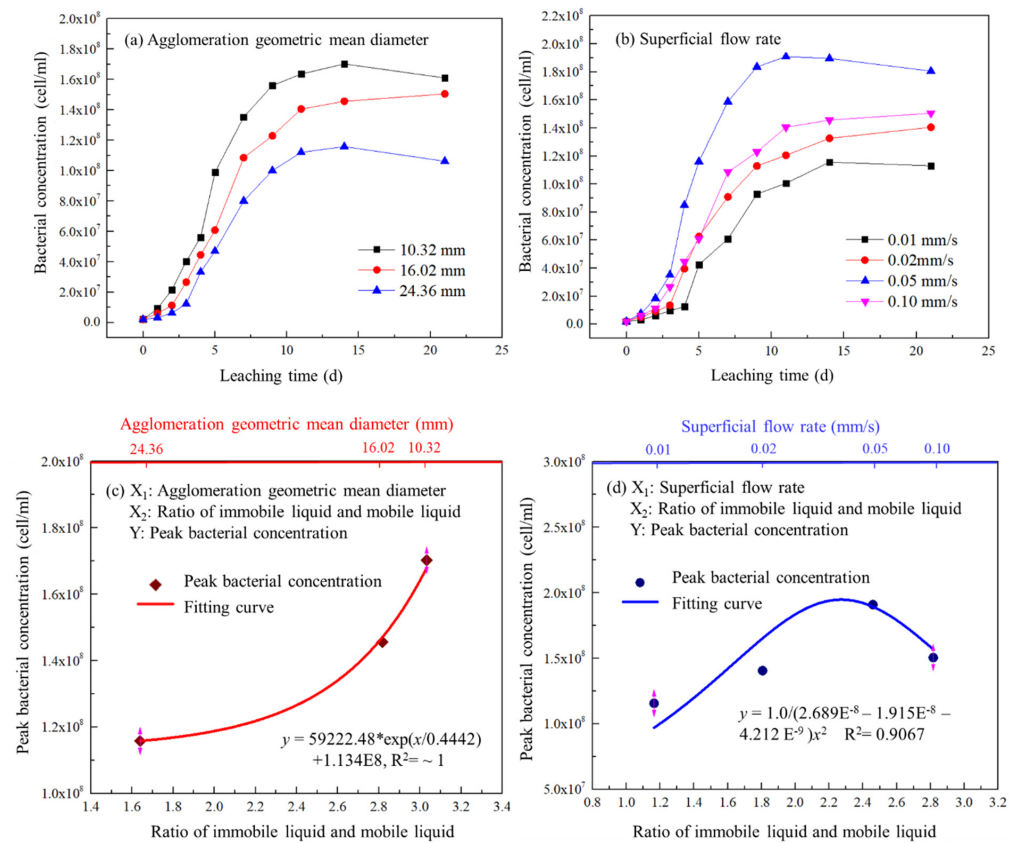


Figure 4. Bacterial concentration with leaching time under different packed and irrigation condition.

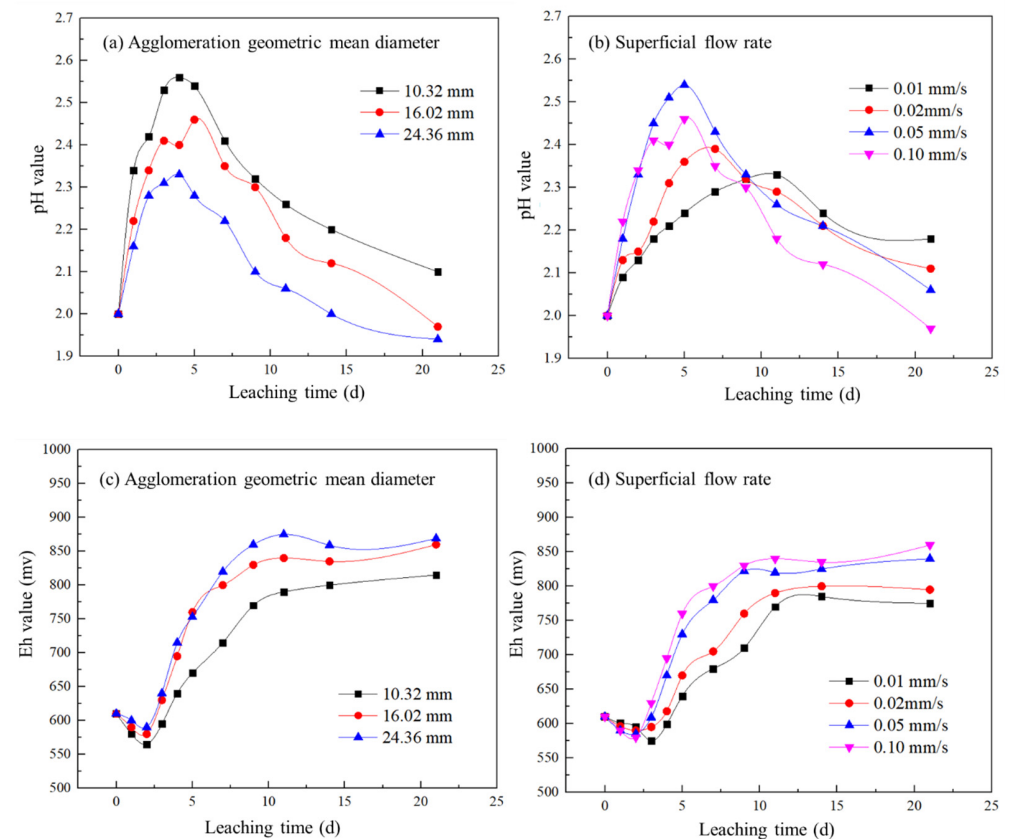
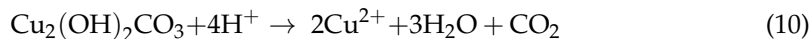


Figure 5. pH/Eh value with leaching time under the different packed and irrigation condition.

In the early leaching period (0–5 days), the pH value reaches nearly 2.60, and oxidation reduction potential (ORP) is generally lower than 650 mV (Figure 5), which corresponds with undesirable copper extraction rate (Figure 3). In the leaching process,  $H^+$  is consumed by the copper oxides and alkaline gangues [32], the acidic leaching of copper oxides is shown in Equation (10). The Eh value increased to 750–850 mV after 10 days of leaching, and the copper minerals are quickly dissolved and leached, which is clearly echoed with a surge increase of copper extraction rate (Figure 3) and bacterial concentration (Figure 4).



In copper sulfides leaching, the  $Fe^{3+}$  is reduced to produce passivation substances such as jarosite, polysulfide, etc. [33,34], and the  $S^{2-}$  is oxidized to produce  $S^0$  and sulfate ions, which promotes the formation of  $H_2SO_4$  (Equation (11)).



These finding also inferred that the pH/Eh heavily affects the leaching, where the higher ORP promotes the mineral dissolutions. Combining with the existing research [35–37], this indicates that ORP affects the intermediate products formation, so it could limit the solute transfer and bioleaching efficiency. Referring to previous studies on liquid retention and hysteresis behavior, it clear that the liquid holdup of unsaturated ore packed beds is higher under a higher  $u$  or a smaller  $R_g$  condition; therefore, combining with results of Figure 5, the ORP is higher in agglomerated heaps where the immobile liquid has a higher proportion, especially in late leaching stage (Figure 5d).

### 3.2. Dynamic Liquid Retention Behavior under Different Leaching Condition

#### (1) Effect of geometric mean diameter ( $R_g$ ) on dynamic liquid retention

To clearly reveal the dynamic liquid retention from the solute transfer, mobile and immobile liquid condition at 0 and 21 days are comparatively discussed in this paper. Figure 6a shows the effect of geometric mean diameter ( $R_g$ ) of WAs on dynamic liquid retention. The ratio of immobile liquid and mobile liquid ( $\eta$ ) continuously changes, and it represents the dynamics liquid retention during the agglomerated column leaching.

Figure 6a shows that if geometric mean diameter of packed WAs is fixed, the  $\eta$  decreases accompanied with leaching reaction. For instance, in the heaps packed by 10.32 mm agglomerations, the proportion of mobile liquid increases from 24.8% of leaching 0 d to 30.9% of 21 d leaching, with a net increase of 4.1%. It speculates that the bio/chemical leaching reaction leads to mineral interface damage, pore throat expansion, and even fluid flow path reconstruction, which promotes mobile fluid paths development, and then it manifests as the proportion increases of mobile fluid after leaching. Further, after the leaching reaction, the increase of mobile liquid proportion is more obvious in the agglomerated heap packed by the small-grained agglomerations. This is consistent with the experimental phenomenon that the pore structure in fine-grained agglomerated heap is well developed. Thus, the flow path is normally well expanded and not only along the former liquid breakthrough paths, which is easy to potentially interfere by leaching reactions and mineral dissolution. However, there is a fact not affected by leaching reaction, namely, the  $\eta$  will gradually decrease if the  $R_g$  of spherical agglomeration feeds increases. As seen in Figure 6a, the  $\eta$  of day 0 decreases from 3.672 to 1.629; similarly, the  $\eta$  of day 21 also decreases from 2.922 to 1.521. This means that, although mineral dissolution could accelerate the flow paths development and increase the mobile liquid flow as a result [38,39], the leaching reaction only weakly affects  $\eta$  and cannot fundamentally subvert the state of liquid retention in the agglomerated heaps. Thus, the liquid retention of agglomerated heaps is more sensitive to geometric mean diameter than leaching reaction. This infers that it is easier to control liquid holdup by regulating the packed feed diameter of WAs, rather than regulating the leaching reaction especially in industrial-scale leaching operation.

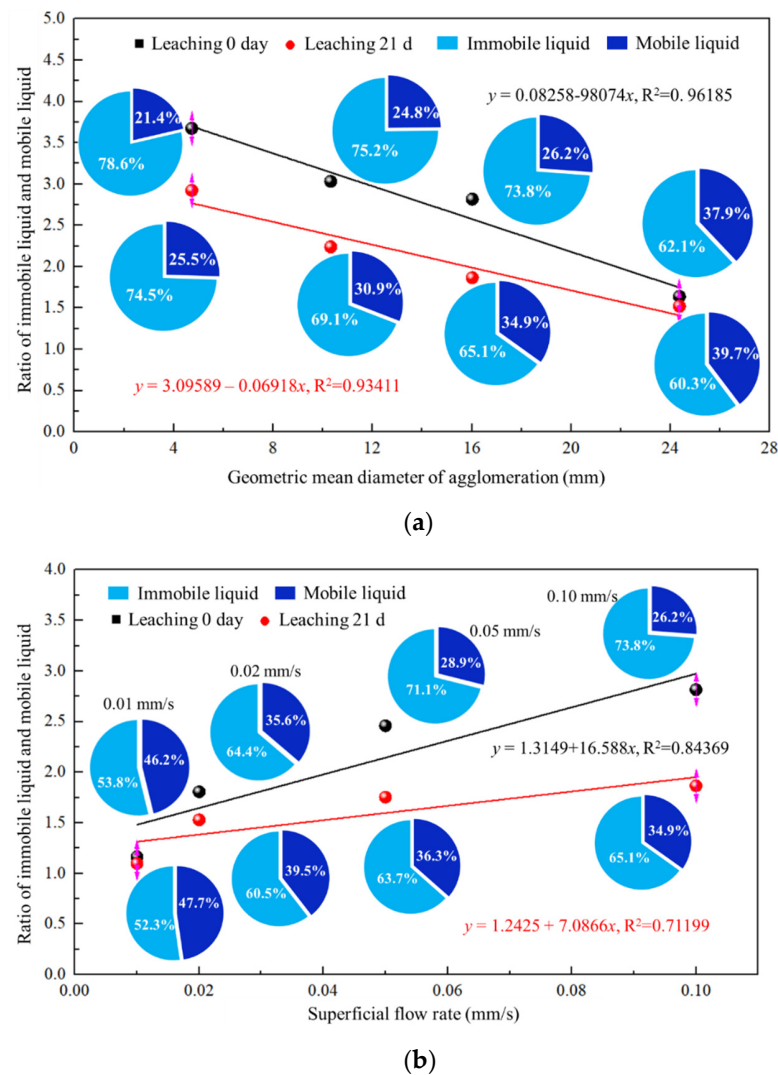


**Figure 6.** Ratio of immobile and mobile liquid under different geometric mean diameter and superficial flow rate. (a) Effect of different geometric mean diameter, (b) Effect of superficial flow rate.

**(2) Effect of superficial flow rate ( $u$ ) on dynamic liquid retention**

Under the co-effects of capillary and gravity forces, the encapsulated liquid film on the agglomeration surface forms the potential fluid paths to promote liquid (or solute) transportation, while the incomplete liquid film causes intermittent liquid retention. The former liquid film is closely related to mobile liquid, and the latter liquid film is closely related to the immobile liquid in the agglomerated heaps. The corresponding relationship between the superficial flow rate ( $u$ ) and ratio of immobile and mobile liquid ( $\eta$ ) is shown in Figure 6b.

The leaching reaction promote the proportion of mobile liquid, eventually making the immobile liquid and mobile liquid to be more balanced. As Figure 6b shows, the  $\eta$  is positively related to  $u$  during the whole leaching process. In other words, the liquid exists as mobile liquid in agglomerated heaps instead residents in the stagnant regions, especially under a lower  $u$ . This does not mean that the mobile liquid is dominant, but it infers that the proportion of mobile liquid can be significantly increased when a lower  $u$  introduced. Taking the leaching on day 21 as an example, the mobile liquid occupied 34.9% at 0.10 mm/s; however, the mobile liquid only occupied 47.7% at 0.01 mm/s. This is because that the preferential flow paths quickly appear and the liquid retention easily reach the steady-state at a higher  $u$  (0.10 mm/s), leading to extensive unsaturated areas distributed in agglomerated heaps. Moreover, no matter how high  $u$  is, the  $\eta$  will certainly decrease accompanied with the mineral dissolution

reactions. It has also been demonstrated that the leaching reaction could enlarge the flow paths and promote the proportion of mobile liquid as a result [40,41]. This decreasing of  $\eta$  is more pronounced at a higher  $u$ . Taking the 0.1 mm/s condition as an example,  $\eta$  significantly decreases from 2.816 to 1.866, and the net reduction is 0.95. However, the net reduction of  $\eta$  is only 0.067 at 0.01 mm/s, which is much lower than the value of the 0.10 mm/s condition.

### 3.3. Response of Solute Transport to Dynamic Liquid Retention of Agglomerated Heaps

#### (1) Effect of superficial flow rate

To better reveal the solute transport under the dynamic liquid spreading condition, the effect of irrigation condition, packed feed types, and agglomeration geometric mean diameter on solute transport behavior are considered in this paper, respectively. Figure 7a,b shows the effect of superficial flow rate ( $u$ ) on the overflow conductivity and residence time distribution (RTD) with irrigation time.

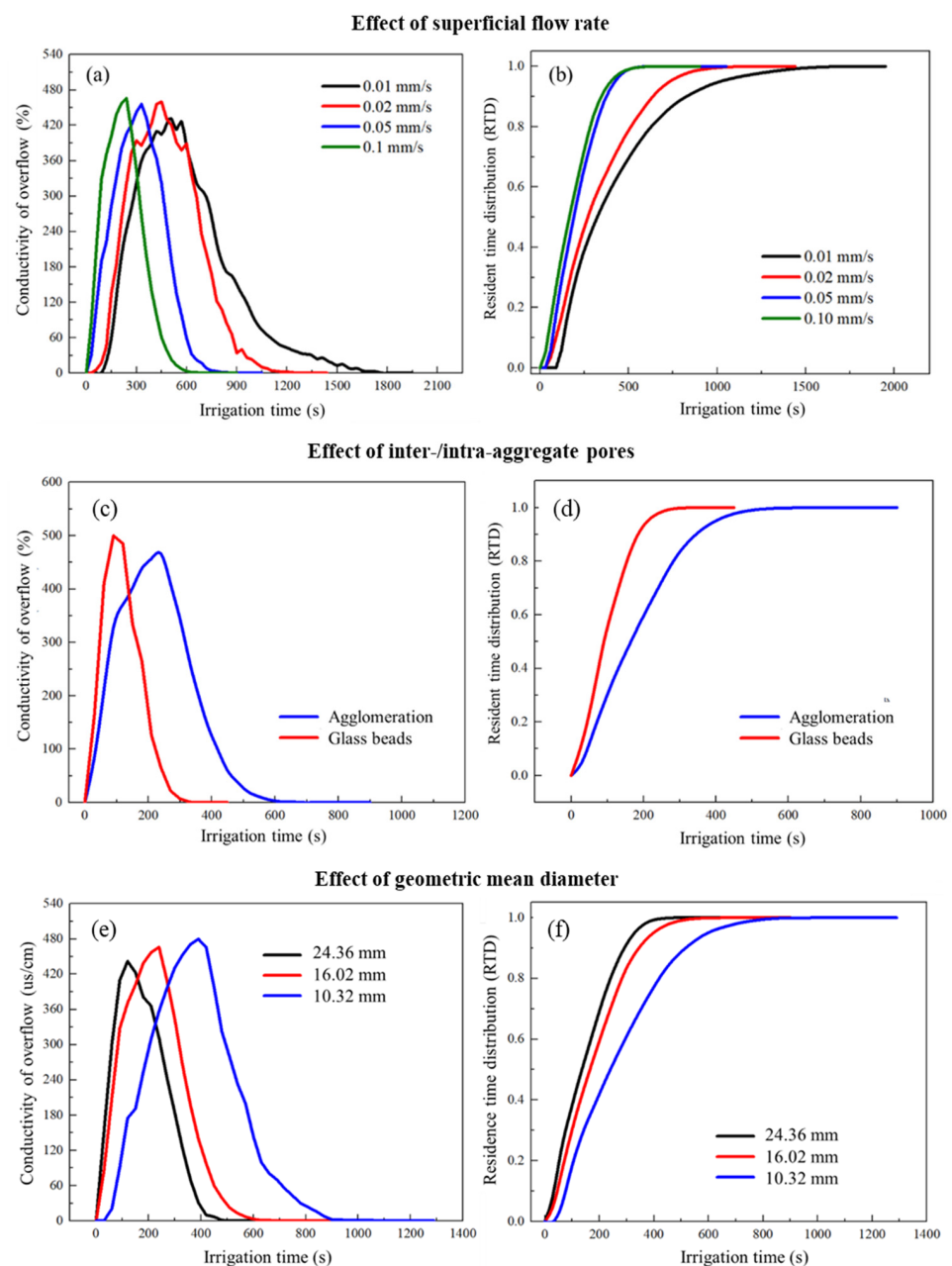


**Figure 7.** Effect of superficial flow rate, inter-/intra- particle porosity, geometric mean diameter on the overflow conductivity and RTD curve with irrigation time.

In Figure 7a, the appearance time of the conductivity pulse peak gradually lags as  $u$  decreases. Specifically, under 0.10 mm/s condition, the peak conductivity value of overflow is 466  $\mu\text{s}/\text{cm}$  at 240 s; when the  $u$  is reduced to 0.01 mm/s, the similar peak conductivity of overflow is obtained. In addition, based on the slope of the curve, the increasing and decreasing process of the overflow liquid conductivity at high  $u$  (0.10 mm/s) are almost symmetrical, but a “dragging phenomenon” is observed under low  $u$  (0.01 mm/s). This indicates that the solute is quickly washed away from the leaching reaction system at high  $u$  (0.10 mm/s), but slowly diffuses and stagnates in the pores/voids at low  $u$  (0.01 mm/s). The liquid dragging is mainly caused by coupled effects of adhesion forces and cohesion forces, which is recognized as the hysteresis behavior [42,43]. The degree of hysteresis is heavily influenced by the interaction surface features (contact angle, surface roughness, etc.) and wettability condition.

As seen in Equations (5) and (6), the residence time distribution (RTD) is shown in Figure 7b. The breakthrough time of solute pulse is positively proportional to the irrigation rate, which decreases from 120 s (0.01 mm/s) to 30 s (0.1 mm/s). Due to the consumed time of the liquid, breakthrough is closely related to the appearance time of preferential flow paths. This means that the shorter the breakthrough time is, the faster liquid retention steady-state reaches. Besides, based on the RTD curve, the solute residence time is around 660 s at 0.01 mm/s, which is much lower than 1770 s at 0.10 mm/s. It is inferred that the ionic solute stagnates for a longer time at a low  $u$  (0.01 mm/s), which is caused by a more developed capillary diffusion under a slow flow rate. These findings also give a guidance for an industrial agglomerated heap, namely, advisably decreasing the irrigation rate (or  $u$ ) could enhance capillary diffusion and promote mass transfer. In contrast, increasing the irrigation rate (or  $u$ ) could quickly recycle the reserved valuable ionic solutes if the leaching reaction is carried out.

### (2) Effect of inter-/intra-aggregate pores

Some previous studies have considered how the developments of inter- and intra-pores affect the retention potential of unsaturated packed beds. This paper focuses on the agglomerated heaps and promotes the understanding of inter-/intra-pores effects on solute transfer via pulse conductivity. Figure 7c,d indicates the effect of inter-/intra-aggregate pores on overflow conductivity with irrigation time via different packed feeds (glass beads, and WAs).

The results of Figure 7c show that consumed time of solute transports is 90 s in glass beads heap, which is much lower than 240 s in heaps of WAs. The intra-porosity of solid glass beads heap is 0%, which is far below that of agglomerated heaps. Based on Figure 7d, the RTD curve implies that the residence time of glass beads is 330 s, which is lower than the residence time (660 s) of agglomerated heaps. This fact confirms that the intra-pores promote liquid hysteresis behavior, strengthen the capillary diffusion, and cause more solutes to stagnate in the agglomerated heaps where the intra- and inter-pores are both well developed. Similarly, it is known the intra-porosity of crushed ore heaps is not as well developed as agglomerated heaps. Hence, this also explains why agglomerated heaps have better liquid holdup and leaching efficiency than crushed ore heaps.

### (3) Effect of geometric mean diameter

Based on previous studies, the development of intra-/inter-pores is very important for liquid hysteresis. Figure 7e,f shows the potential effect of geometric mean diameter on the overflow conductivity and solute residence time features.

Figure 7e indicated that the peak conductivity value and residence time of solute transport is heavily affected by the geometric mean diameter of packed feeds. The peak conductivity value is 480  $\mu\text{s}/\text{cm}$  (in 10.32 mm agglomerated heaps), which is much higher than 442  $\mu\text{s}/\text{cm}$  (in 24.36 mm agglomerated heaps). More potential flow paths exist in the agglomerated heaps with well-developed pores. Thus, the liquid dispersion and solute transport is more complicated and harder to predict. Based on the results shown in Figure 7f in this paper, the solute residence time in the heaps packed by 10.32 mm

WAs is highest (1050 s); in contrast, it decreases to 480 s in the heaps packed by 24.36 mm WAs. This obvious difference in residence time suggests that the well-developed pore structure (smaller diameter agglomerations) could have a higher liquid holdup value of (residual) steady-state and obvious hysteresis phenomenon. Thus, in the feed dumping procedure [44–46], appropriately reducing the feeds diameter of WAs effectively improves the heaps' porosity, ameliorating liquid retention, and solute transport.

#### 4. Conclusions

This paper reveals the potential effects of leaching reaction on dynamic liquid retention and hysteresis behavior of agglomerated heaps. The main findings are as follow:

- (1) The dynamic liquid holdup is carefully quantified via RILRCS system, the copper extraction rate is higher when the WAs diameter is smaller (10.32 mm). Increasing the surficial flow rate could decrease the ratio of immobile and mobile liquid ( $\eta$ );
- (2) The RTD results show that increasing intra- porosity of agglomerated heaps and superficial flow rate could extend solute residence time. However, the excessive superficial flow rate easily results in preferential flow formation and low copper leaching rate;
- (3) Leaching reaction tends to promote the proportion of mobile liquid, and increase the peak liquid holdup value. The leaching reaction tends to develop the flow paths, which is mainly shown as the reduction of  $\eta$ .

From the results described in this paper, it can be seen that bioleaching reactions have a significant impact on liquid holding behavior. The concentration change of solute type caused by mineral reaction, reaction passivation, and interface liquid-solid contact angle will be the focus of follow-up research.

**Author Contributions:** Conceptualization, L.W. and X.Z.; methodology, L.W., X.Z.; software, X.Z. and Z.Y.; validation, L.W. and S.Y.; data curation, L.W. and Z.Y.; writing—original draft preparation, L.W., X.Z. and Z.Y.; writing—review and editing, L.W. and S.Y.; visualization, L.W. and W.L.; supervision, S.Y., L.W. and W.L.; project administration, L.W. and S.Y.; funding acquisition, L.W. and S.Y. All authors have read and agreed to the published version of the manuscript.

**Funding:** This research was funded by the Program of the National Natural Science Foundation of China (52204124,52034001); China National Postdoctoral Program for Innovative Talents (BX20220036), China Postdoctoral Science Foundation (2022M710356), Fundamental Research Funds for the Central Universities (FRF-IDRY-21-010, QNXM20220001); open project of State Key Laboratory of Coal Mine resources and safety mining (SKLCRSM22KF006); open project of State Key Laboratory of Safety and Health for Metal Mines (2021-JSKSSYS-01), Open Project of Key Laboratory of Green Chemical Engineering Process of Ministry of Education (GCP202108).

**Data Availability Statement:** The data are not publicly available due to confidential reasons.

**Acknowledgments:** Thanks for the great efforts of editors and reviewers.

**Conflicts of Interest:** The authors declare no conflict of interest.

#### References

1. Yin, S.; Wang, L.; Kabwe, E.; Chen, X.; Yan, R.; An, K.; Zhang, L.; Wu, A. Copper Bioleaching in China: Review and Prospect. *Minerals* **2018**, *8*, 32. [[CrossRef](#)]
2. Rawlings, D.E. Heavy Metal Mining Using Microbes. *Annu. Rev. Microbiol.* **2002**, *56*, 65–91. [[CrossRef](#)]
3. Lizama, H.M. How Copper Dump Leaching Works. *Miner. Eng.* **2021**, *171*, 107075. [[CrossRef](#)]
4. van Staden, P.J.; Petersen, J. Towards Fundamentally Based Heap Leaching Scale-Up. *Miner. Eng.* **2021**, *168*, 106915. [[CrossRef](#)]
5. Yin, S.; Wang, L.; Chen, X.; Wu, A. Agglomeration and Leaching Behavior of Copper Oxides with Different Chemical Binders. *Int. J. Miner. Metall. Mater.* **2021**, *28*, 1127–1134. [[CrossRef](#)]
6. van Staden, P.J.; Petersen, J. The Effects of Simulated Stacking Phenomena on the Percolation Leaching of Crushed Ore, Part 2: Stratification. *Miner. Eng.* **2019**, *131*, 216–229. [[CrossRef](#)]
7. van Staden, P.J.; Petersen, J. The Effects of Simulated Stacking Phenomena on the Percolation Leaching of Crushed Ore, Part 1: Segregation. *Miner. Eng.* **2018**, *128*, 202–214. [[CrossRef](#)]

8. Lewandowski, K.A.; Eisele, T.C.; Komar Kawatra, S. Agglomeration for Copper Heap Leaching. In Proceedings of the XXV International Mineral Processing Congress 2010, Brisbane, Australia, 6–10 September 2010.
9. Wang, L.; Yin, S.; Wu, A.; Chen, W. Effect of Stratified Stacks on Extraction and Surface Morphology of Copper Sulfides. *Hydrometallurgy* **2020**, *191*, 105226. [[CrossRef](#)]
10. Wang, L.; Yin, S.; Wu, A.; Chen, W. Synergetic Bioleaching of Copper Sulfides Using Mixed Microorganisms and Its Community Structure Succession. *J. Clean. Prod.* **2020**, *245*, 118689. [[CrossRef](#)]
11. Maghsoudy, S.; Bakhtiari, O.; Maghsoudy, S. Tortuosity Prediction and Investigation of Fluid Flow Behavior Using Pore Flow Approach in Heap Leaching. *Hydrometallurgy* **2022**, *211*, 105868. [[CrossRef](#)]
12. Fernando, W.A.M.; Ilankoon, I.M.S.K.; Rabbani, A.; Chong, M.N. Applicability of Pore Networks to Evaluate the Inter-Particle Flow in Heap Leaching. *Hydrometallurgy* **2020**, *197*, 105451. [[CrossRef](#)]
13. Mitchell, R.J.; Mayer, A.S. A Numerical Model for Transient-Hysteretic Flow and Solute Transport in Unsaturated Porous Media. *J. Contam. Hydrol.* **1998**, *30*, 243–264. [[CrossRef](#)]
14. Midoux, N.; Charpentier, J.C. Apparent Diffusivity and Tortuosity in a Liquid-Filled Porous Catalyst Used for Hydrodesulfuration of Petroleum Products. *Chem. Eng. Sci.* **1973**, *28*, 2108–2111. [[CrossRef](#)]
15. Shi, Z.; Zhang, Y.; Liu, M.; Hanaor, D.A.H.; Gan, Y. Dynamic Contact Angle Hysteresis in Liquid Bridges. *Colloids Surf. A Physicochem. Eng. Asp.* **2018**, *555*, 365–371. [[CrossRef](#)]
16. Fernando, W.A.M.; Ilankoon, I.M.S.K.; Rabbani, A.; Yellishetty, M. Inter-Particle Fluid Flow Visualisation of Larger Packed Beds Pertaining to Heap Leaching Using X-ray Computed Tomography Imaging. *Miner. Eng.* **2020**, *151*, 106334. [[CrossRef](#)]
17. Li, Z.; Liu, D.; Cai, Y.; Ranjith, P.G.; Yao, Y. Multi-Scale Quantitative Characterization of 3-D Pore-Fracture Networks in Bituminous and Anthracite Coals Using FIB-SEM Tomography and X-ray M-CT. *Fuel* **2017**, *209*, 43–53. [[CrossRef](#)]
18. Wang, L.; Yin, S.; Wu, A. Visualization of Flow Behavior in Ore Segregated Packed Beds with Fine Interlayers. *Int. J. Miner. Met. Mater.* **2020**, *27*, 900–909. [[CrossRef](#)]
19. Muzemder, A.S.H.; Singh, K. Intra-Pore Tortuosity and Diverging-Converging Pore Geometry Controls on Flow Enhancement Due to Liquid Boundary Slip. *J. Hydrol.* **2021**, *598*, 126475. [[CrossRef](#)]
20. Or, D.; Tuller, M. Liquid Retention and Interfacial Area in Variably Saturated Porous Media: Upscaling from Single-Pore to Sample-Scale Model. *Water Resour. Res.* **1999**, *35*, 3591–3605. [[CrossRef](#)]
21. Tuller, M.; Or, D. Unsaturated Hydraulic Conductivity of Structured Porous Media. *Vadose Zone J.* **2002**, *1*, 14–37. [[CrossRef](#)]
22. Or, D.; Tuller, M. Flow in Unsaturated Fractured Porous Media: Hydraulic Conductivity of Rough Surfaces. *Water Resour. Res.* **2000**, *36*, 1165–1177. [[CrossRef](#)]
23. Fagan-Endres, M.A.; Harrison, S.T.L.; Johns, M.L.; Sederman, A.J. Magnetic Resonance Imaging Characterisation of the Influence of Flowrate on Liquid Distribution in Drip Irrigated Heap Leaching. *Hydrometallurgy* **2015**, *158*, 157–164. [[CrossRef](#)]
24. Ilankoon, I.M.S.K.; Neethling, S.J. The Effect of Particle Porosity on Liquid Holdup in Heap Leaching. *Miner. Eng.* **2013**, *45*, 73–80. [[CrossRef](#)]
25. Ilankoon, I.M.S.K.; Neethling, S.J. Hysteresis in Unsaturated Flow in Packed Beds and Heaps. *Miner. Eng.* **2012**, *35*, 1–8. [[CrossRef](#)]
26. Wang, L.; Yin, S.; Deng, B. Understanding the Effect of Stepwise Irrigation on Liquid Holdup and Hysteresis Behavior of Unsaturated Ore Heap. *Minerals* **2021**, *11*, 1180. [[CrossRef](#)]
27. Wang, L.; Yin, S.; Wu, A. Ore Agglomeration Behavior and Its Key Controlling Factors in Heap Leaching of Low-Grade Copper Minerals. *J. Clean. Prod.* **2020**, *279*, 123705. [[CrossRef](#)]
28. Wang, L.; Yin, S.; Deng, B.; Wu, A. Copper Sulfides Leaching Assisted by Acidic Seawater-Based Media: Ionic Strength and Mechanism. *Miner. Eng.* **2022**, *175*, 107286. [[CrossRef](#)]
29. Ilankoon, S.K. Hydrodynamics of Unsaturated Particle Beds Pertaining to Heap Leaching. Ph.D. Thesis, Imperial College London, London, UK, 2012.
30. Toye, D.; Marchot, P.; Crine, M.; Pelsser, A.M.; L’Homme, G. Local Measurements of Void Fraction and Liquid Holdup in Packed Columns Using X-ray Computed Tomography. *Chem. Eng. Process. Process Intensif.* **1998**, *37*, 511–520. [[CrossRef](#)]
31. Hashemzadeh, M. Copper Leaching in Chloride Media with a View to Using Seawater for Heap Leaching of Secondary Sulfides. Ph.D. Thesis, The University of British Columbia, University Endowment Lands, BC, Canada, 2020.
32. Thomas, M. Understanding Gangue Acid Consumption in Copper Sulfide Heap Leaching: Predicting the Impact of Carbonates, Silicates and Secondary Precipitates. *Miner. Eng.* **2021**, *171*, 107090. [[CrossRef](#)]
33. Dreisinger, D. Copper Leaching from Primary Sulfides: Options for Biological and Chemical Extraction of Copper. *Hydrometallurgy* **2006**, *83*, 10–20. [[CrossRef](#)]
34. Tshilombo, A.F. Mechanism and Kinetics of Chalcopyrite Passivation and Depassivation during Ferric and Microbial Leaching. Ph.D. Thesis, The University of British Columbia, University Endowment Lands, BC, Canada, 2004.
35. Liu, R.; Hao, X.; Chen, Q.; Li, J. Research Advances of Tetrasphaera in Enhanced Biological Phosphorus Removal: A Review. *Water Res.* **2019**, *166*, 115003. [[CrossRef](#)]
36. Nicol, M.J.; Zhang, S. Anodic Oxidation of Iron(II) and Copper(I) on Various Sulfide Minerals in Chloride Solutions. *Hydrometallurgy* **2016**, *166*, 167–173. [[CrossRef](#)]
37. Nicol, M.J. The Electrochemistry of Chalcopyrite in Alkaline Solutions. *Hydrometallurgy* **2019**, *187*, 134–140. [[CrossRef](#)]
38. Wu, A.; Yin, S.; Qin, W.; Liu, J.; Qiu, G. The Effect of Preferential Flow on Extraction and Surface Morphology of Copper Sulfides during Heap Leaching. *Hydrometallurgy* **2009**, *95*, 76–81. [[CrossRef](#)]

39. Bouffard, S.C.; Dixon, D.G. Investigative Study into the Hydrodynamics of Heap Leaching Processes. *Metall. Mater. Trans. B* **2001**, *32*, 763–776. [[CrossRef](#)]
40. Chen, K.; Yin, W.; Ma, Y.; Yang, B.; Sun, H.; Rao, F.; Liu, J. Microstructure Analysis of Low-Grade Copper Ore Agglomerates Prepared by Geopolymerization. *Hydrometallurgy* **2021**, *200*, 105564. [[CrossRef](#)]
41. Yang, Y.; Yang, Y.; Gao, X.; Petersen, J.; Chen, M. Microstructure Evolution of Low-Grade Chalcopyrite Ores in Chloride Leaching—A Synchrotron-Based X-ray CT Approach Combined with a Data-Constrained Modelling (DCM). *Hydrometallurgy* **2019**, *188*, 1–13. [[CrossRef](#)]
42. Von Fraunhofer, J.A. Adhesion and Cohesion. *Int. J. Dent.* **2012**, *2012*, 951324. [[CrossRef](#)]
43. Extrand, C.W. Contact Angles and Their Hysteresis as a Measure of Liquid-Solid Adhesion. *Langmuir* **2004**, *20*, 4017–4021. [[CrossRef](#)]
44. Zhang, S.; Liu, W.; Granata, G. Effects of Grain Size Gradation on the Porosity of Packed Heap Leach Beds. *Hydrometallurgy* **2018**, *179*, 238–244. [[CrossRef](#)]
45. Ghorbani, Y.; Becker, M.; Mainza, A.; Franzidis, J.P.; Petersen, J. Large Particle Effects in Chemical/Biochemical Heap Leach Processes—A Review. *Miner. Eng.* **2011**, *24*, 1172–1184. [[CrossRef](#)]
46. Zhang, S.; Liu, W. Application of Aerial Image Analysis for Assessing Particle Size Segregation in Dump Leaching. *Hydrometallurgy* **2017**, *171*, 99–105. [[CrossRef](#)]